

Electronic Supplementary Information (ESI)

Nitrogen-doped Open Pore Channeled Graphene Facilitating Electrochemical Performance of TiO₂ Nanoparticles as Anode Materials for Sodium Ion Batteries

Hyun Ae Cha,^{a, d‡} Hyung Mo Jeong,^{b‡} and Jeung Ku Kang^{a, b, c*}

^a Graduate School of Energy, Environment, Water, and Sustainability (EEWS), Korea Advanced Institute of Science and Technology (KAIST), 291 Daehak-ro, Yuseong-gu, Daejeon 305-701, Republic of Korea. E-mail: jeungku@kaist.ac.kr; Fax: +82-42-350-3310; Tel: +82-42-350-3378

^b Department of Materials Science & Engineering, Korea Advanced Institute of Science and Technology (KAIST), 291 Daehak-ro, Yuseong-gu, Daejeon 305-701, Republic of Korea

^c NanoCentury KAIST Institute, Korea Advanced Institute of Science and Technology, 291 Daehak-ro, Yuseong-gu, Daejeon, 305-701, Republic of Korea.

^d Powder & Ceramic Division, Korea Institute of Materials Science (KIMS), 797 Changwondaero, Seongsangu, Changwon, Gyeongnam, 642-831, Republic of Korea

[‡] Hyun Ae Cha and Hyung Mo Jeong contributed equally to this work.

[†] Electronic Supplementary Information (ESI) available: [details of any supplementary information available should be included here]. See DOI: 10.1039/b000000x/

Experimental Details

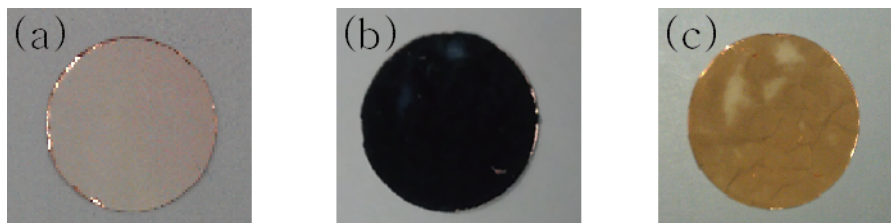
Synthesis of the TNCG: All chemicals and solvents were purchased from Sigma-Aldrich. The CG was prepared by the following procedure. The GO was synthesized from natural graphite powder by a modified Hummer's method.¹ 150 mg of the brown GO was dispersed in 150 ml of distilled water and then exfoliated by ultrasonication using an ultrasonic bath (JAC-2010, Kodo) for 2 h. The product was then transferred to a 500 ml round-bottom flask. 300 mg of KMnO_4 and 1 ml of ammonia solution were added next. After stirring for 0.5 h, the mixed solution was heated in a commercial microwave oven (Daewoo, KR-B200B) for 10 minutes. The resultant solution was stirred with 50 ml of distilled water until it cooled. In this step, the carbon atoms serve as a sacrificial reductant and convert aqueous permanganate (MnO_4^-) to insoluble MnO_2 .² It was then refluxed at 95 °C for 20 h with 1 ml of hydrazine solution (35 wt % in water, Sigma-Aldrich). Finally, the solution was filtered with 500 ml oxalic acid and hydrochloric acid (0.1 M, v/v, 1:1) to remove unreacted ionic impurities, and then washed with distilled water and ethanol several times until reaching the neutral pH. The final product was dried in supercritical CO_2 . Nitrogen-doping for synthesizing the NCG was performed on the prepared samples under 450 °C for 2 h with 10 torr of nitrogen gas (100 sccm) at a rate of 5 °C per minute.

The TNCG was prepared via the following procedure. 0.2 ml of titanium isopropoxide was mixed with 50 mg of NCG in a 15 ml of H_2SO_4 (1 M) solution and ultrasonicated for 1 h. The product was then transferred to a Teflon-lined autoclave (23 ml in capacity). The sealed autoclave was maintained at 130 °C for 12 h. After reaction, the final product was isolated by filtration, rinsed thoroughly with deionized water, and dried at 70 °C under vacuum overnight. The TNCG as a green-black powder was obtained. The BTO nanoparticles were synthesized under the same conditions without the addition of channeled graphene sheets for comparison.

Electrochemical testing: The working electrodes were prepared by mixing the TNCG (75 wt %), carbon black (Super-P, 15 wt %), and poly (vinylidene fluoride) binder (PVdF, 10 wt %) in N-methyl-2-pyrrolidone (NMP) to make a slurry. The slurry was pasted on pure Cu foil (150 μm) using a doctor blade and dried in a vacuum oven at 70 $^{\circ}\text{C}$ overnight. The electrochemical performances of the prepared samples were investigated using a CR2032 type battery assembled in an argon-filled glove box with a pure sodium metal as the counter/reference electrode. The electrolyte used was 1 M NaClO_4 in 1:1 (v/v) ethylene carbonate/diethyl carbonate (EC/DEC) electrolyte. Celgard 2400 polypropylene was used as a separator. Charge-discharge measurements were performed under different current densities in a potential range from 0.01 to 3 V versus Na/Na^+ .

Structure Characterization: The XRD (RIGAKU; D/MAX-2500) spectra were acquired using $\text{CuK}\alpha$ radiation to analyze the crystal structures of the GO, CG, NCG, and TNCG samples. The Raman spectroscopy (excitation, 514 nm, High Resolution Micro Raman/ low temp, PL System, LabRAM HR UV/Vis/NIR PL) measurement was used to investigate the characteristics of GO, CG, NCG and TNCG samples. The morphologies were characterized by the field emission scanning electron microscopy (FESEM, Magellan 400) and HRTEM (JEOL, JEM-ARM200F). The weight portion of the channeled graphene in the TNCG was obtained on the basis of TGA (Thermogravimetry Analyzer, TG 209 F3) measurements. Nitrogen adsorption and desorption isotherms were attained using the Brunauer-Emmett-Teller (BET, Quantachrome) method after degassing the samples at 150 $^{\circ}\text{C}$ for 5 h. The atomic bonding configurations were obtained by XPS (Thermo VG Scientific, Sigma Probe).

Fig. S1 Photographs taken (a) before cycling (b) after cycling of the BTO as an anode for the sodium ion battery. When discharged to 0.01 V (vs Na/Na⁺) after cycling, the half-cell was disassembled to obtain the electrode film. (c) The disassembled electrode film change color after washing out with DIW.



The anatase TiO₂ synthesized by hydrothermal synthesis has a white color. Figure S1a is the slurry of the BTO mixed with the PVdF (10 wt %). Figure S1b shows the disassembled electrode film which has the Ti³⁺ when sodium ion is stored in the TiO₂ after fully being discharged at 0.01 V (Na/Na⁺). Because of the Ti³⁺, the sample has black color. The black color is changed to white after washing out because Ti³⁺ changed to Ti⁴⁺.³

Fig. S2 SEM images of the GO at (a) low and (b) high magnifications.

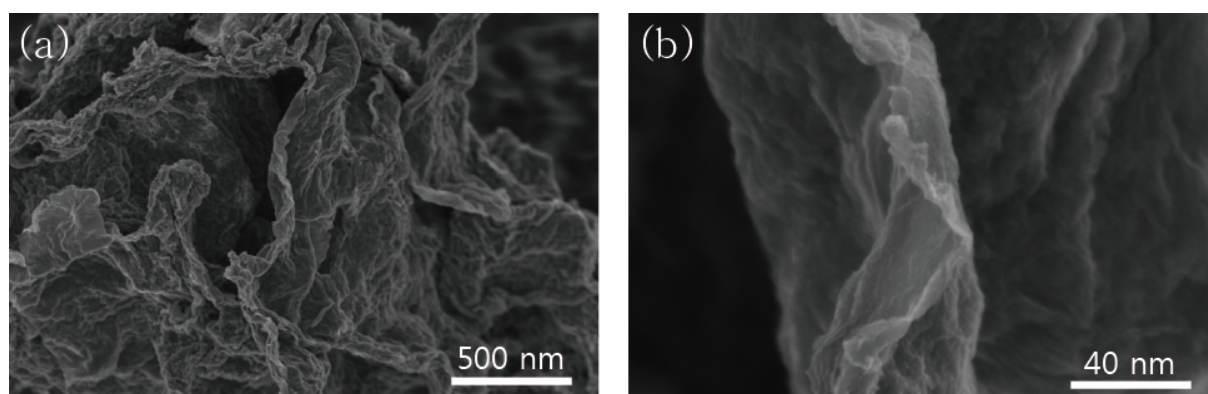
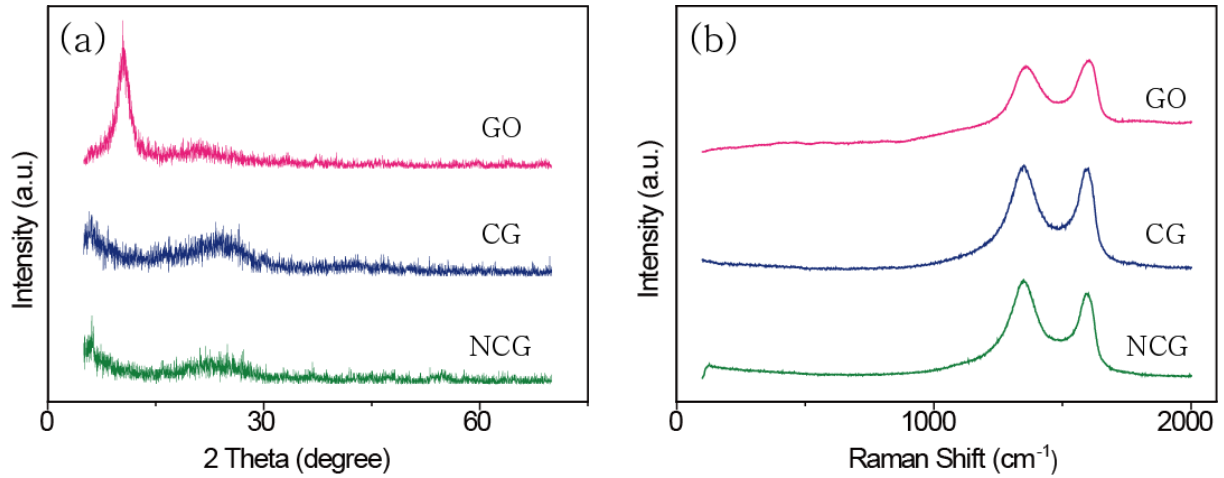


Fig. S2 displays the experimental GO synthesized by the modified Hummer's method analyzed using the FESEM.¹

Fig. S3 (a) XRD patterns of GO, CG and NCG samples. (b) Raman spectra of GO, CG and NCG samples, with an excitation laser wavelength of 514 nm.



The XRD patterns of GO, CG and NCG samples are presented in Figure S3a. The peak at $\sim 10^\circ$ in the GO pattern indicates that the raw graphite has been successfully oxidized to the GO. The patterns of CG and NCG samples contain a very broad reflection at $2\theta = 24^\circ$ (corresponding to d spacing of 0.37 nm). This matches well with that for a graphene sheet. In the Raman analysis (Figure S3b), the D/G intensity ratios of GO and CG samples are 0.95 and 1.03, respectively, indicating that the GO reduces to the graphene. Compared to the CG, the high intensity of the D band (at 1350 cm^{-1} for the disordered structure, the D/G intensity: 1.12) of the NCG suggests the presence of more defects on the NCG by nitrogen-doping.

Fig. S4 Pore distribution of (a) Graphene, (b) CG, and (c) TNCG samples.

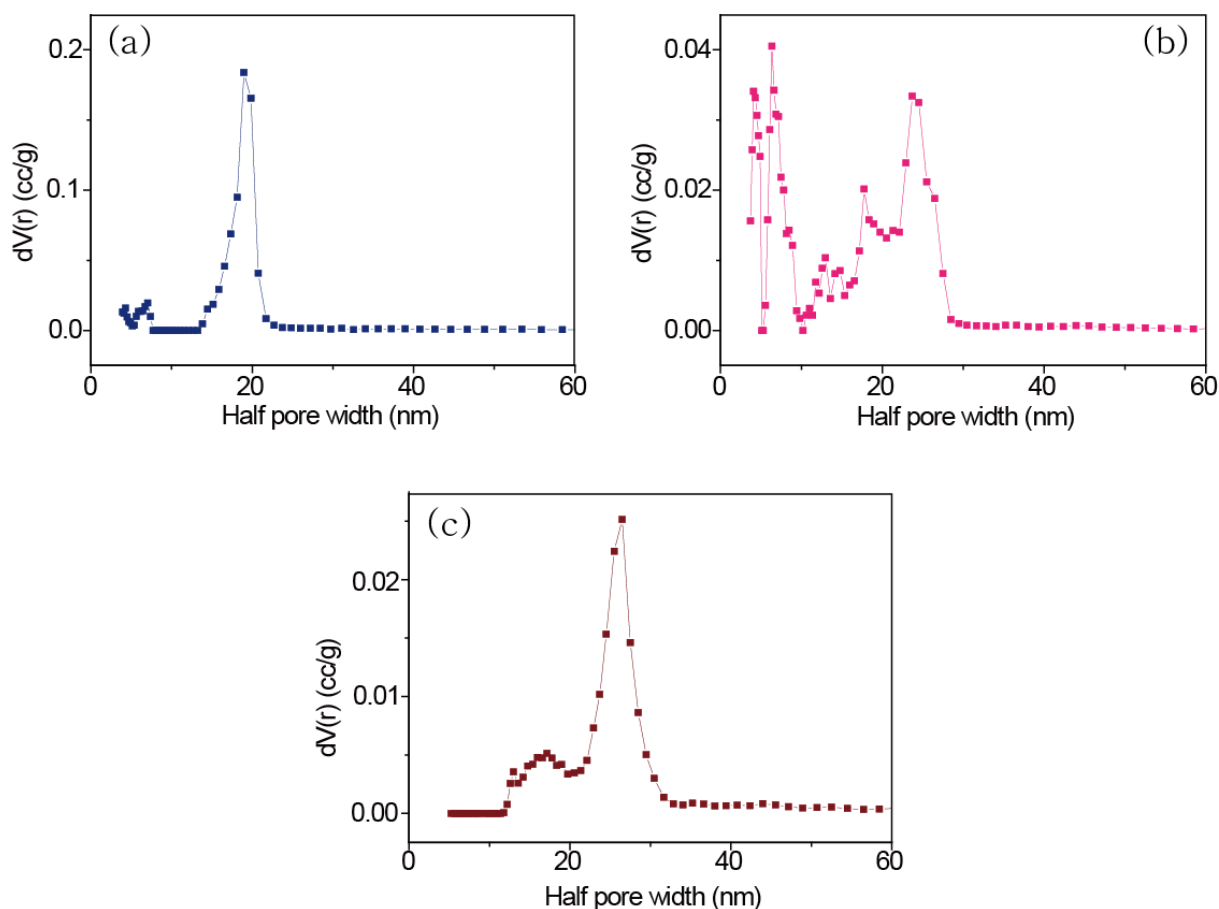


Fig. S4 shows the pore distribution of (a) Graphene, (b) CG and (c) TiO₂/nitrogen-doped graphene composite samples. The pore size distributions of graphene, CG, and TiO₂/nitrogen-doped graphene composite samples were obtained from a micropore plot using the NLDFIT method. As seen from the plot, the graphene displays a half pore width of only 19 nm, whereas the CG sample display half pore widths at 24 nm and 5 nm. Pores of 5 nm size were synthesized using oxidation-etching. As pores are formed in the graphene, the pore volume at a half pore width of around 20 nm is reduced because wrinkles of graphene are decreased by introducing pores. The TiO₂/nitrogen-doped graphene displays a half pore width of only around 25 nm in Fig. S4c. The result reveals that there are no pores in the TiO₂/nitrogen-doped graphene composites in contrast with the pore distribution of the TNCG.

Fig. S5 Thermal behavior of the TNCG.

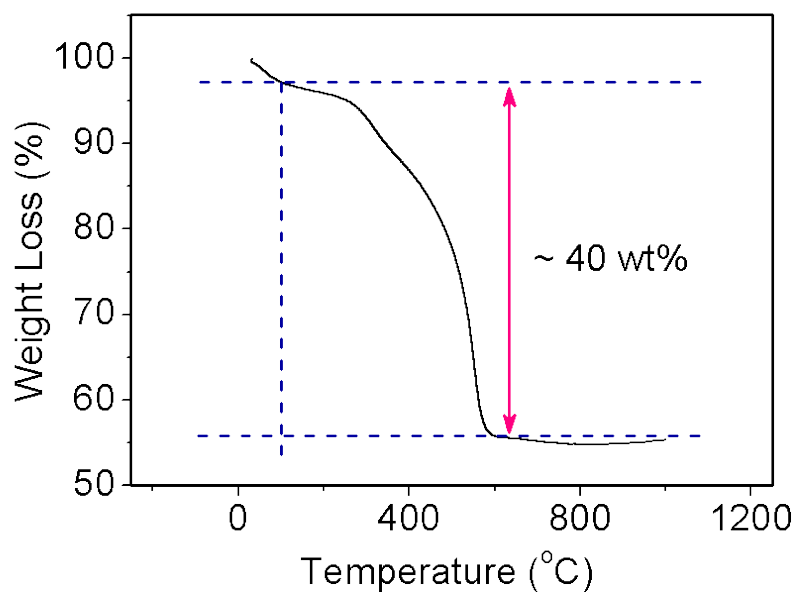


Fig. S5 shows thermogravimetric analysis (TGA) results of the TNCG. The weight loss of 2.5 % below 100 °C is likely due to evaporation of the absorbed moisture, which is common for materials with large surface area. An apparent large weight loss can be observed at ~500 °C and the total amount of the graphene presented in the composite is measured to be ~40 wt % up to 600 °C.

Fig. S6 Cyclic voltammetric measurements of the BTO and the NCG.

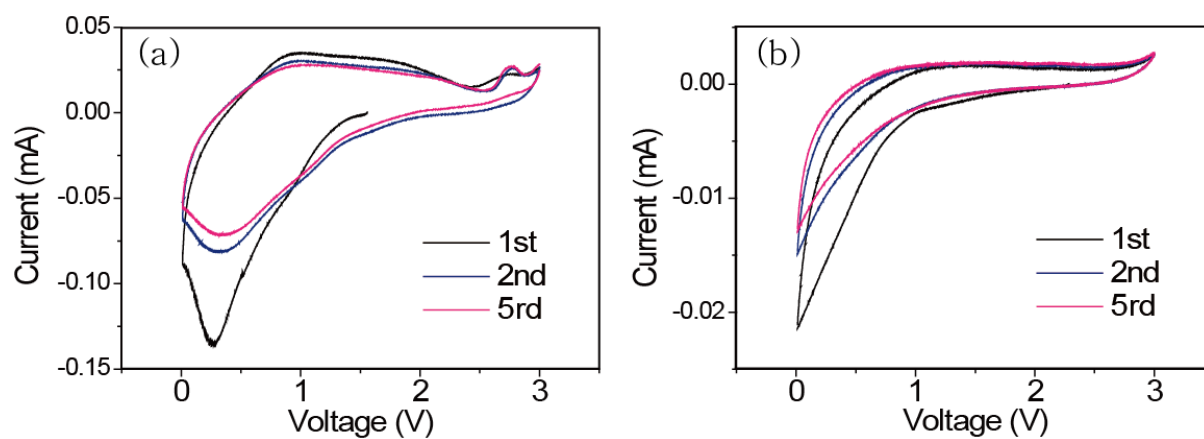
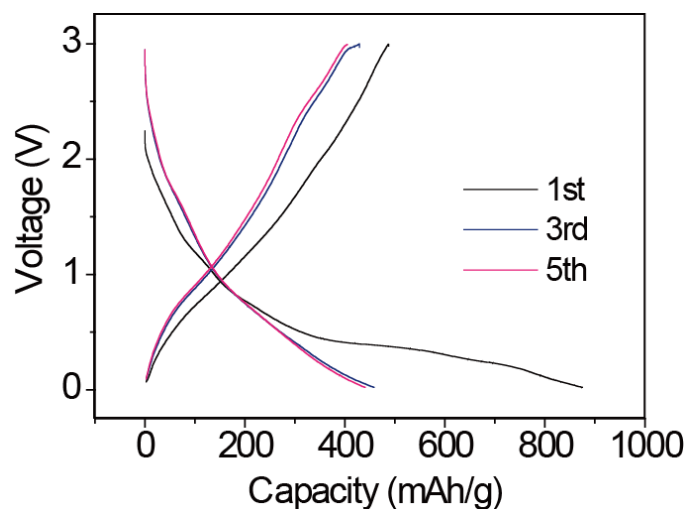


Fig. S6 shows cyclic voltammograms of the BTO and NCG electrodes obtained at a scan rate of 0.1 mV s^{-1} from the open circuit voltage to $0.01 \text{ V vs Na/Na}^+$.

Fig. S7 Charge-discharge profile of TNCG samples.



The electrode shows the charge and discharge profiles of the TNCG at a current density of 50 mA g⁻¹. The first cycle of the electrode exhibited irreversible capacity attributed to the formation of the SEI layer. It is notable that the measured capacity is much higher than other reported values for Na-ion batteries based on an intercalation reaction, such as amorphous TiO₂ (150 mAh g⁻¹ at a current density of 50 mA g⁻¹)⁴, Na₂Ti₃O₇ (177 mAh g⁻¹ at a current density of 35.6 mA g⁻¹)⁵, and Li₄Ti₅O₁₂ (125 mAh g⁻¹ at a 0.2 C rate)⁶.

Fig. S8 The EIS spectra of pristine graphene (G) and channeled graphene (CG) electrodes.

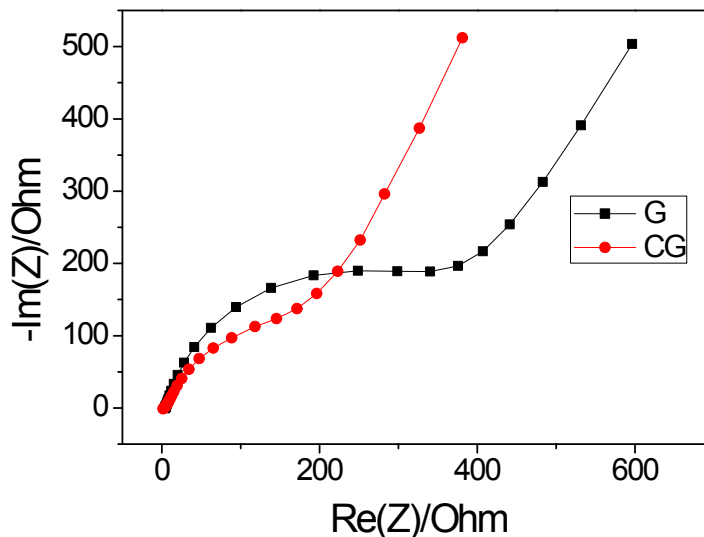


Fig. S8 plots the electrochemical impedance spectroscopy (EIS) curves of graphene (G) and channeled graphene (CG) samples. The radius for the semicircles of the CG electrode in the high-medium frequency region is smaller than that of the G electrode, suggesting that the charge-transfer resistance of the CG is lower than that of the G electrode. This verifies that the open channeled on graphene sheets improve the ion accessibility and conductivity of the overall electrode.

Fig. S9 The EIS of BTO, TCG and TNCG electrodes.

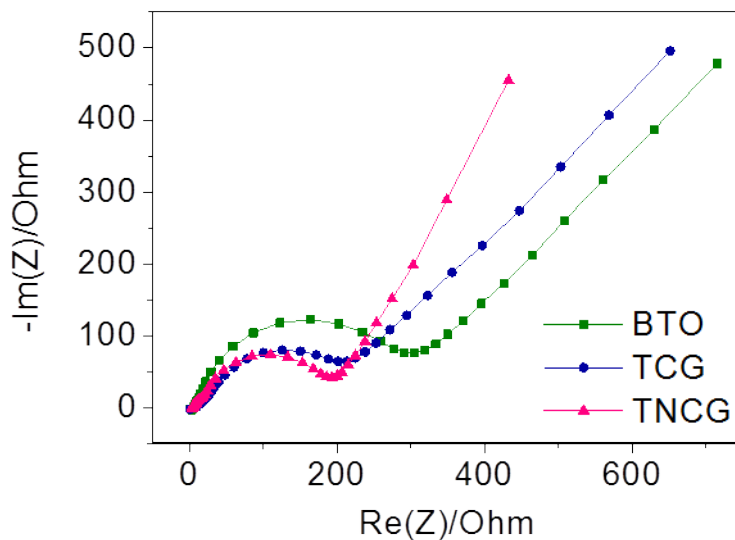


Fig. S9 plots the electrochemical impedance spectroscopy (EIS) curves of BTO, TCG and TNCG samples. The radius for the semicircles of the TCG electrode in the high-medium frequency region is smaller than that of the BTO electrode, suggesting that the charge-transfer resistance of the TCG is lower than that of the BTO electrode. This verifies that the open channeled graphene sheets improve the conductivity of the overall electrode by forming the composite electrode. Also, it is found that the charge-transfer resistance of the TNCG is lower than that of the TCG electrode. This supports that the nitrogen-doping in the open channeled graphene sheets improve the conductivity of the electrode.

Fig. S10 Cycling performances of graphene and NCG samples.

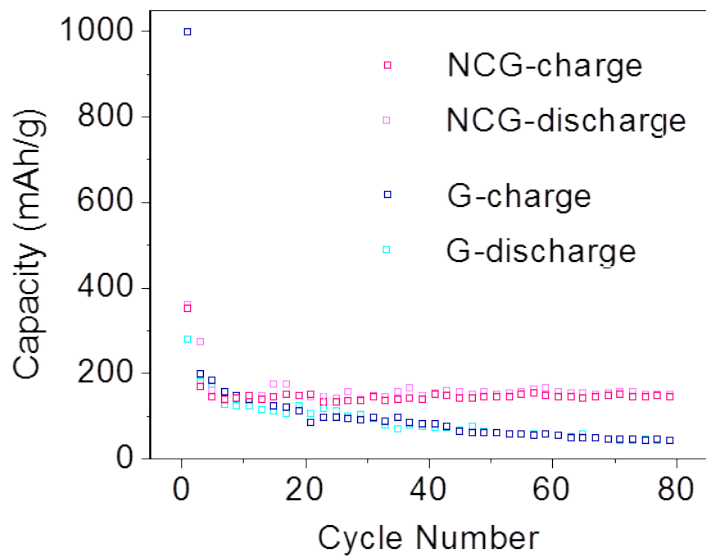
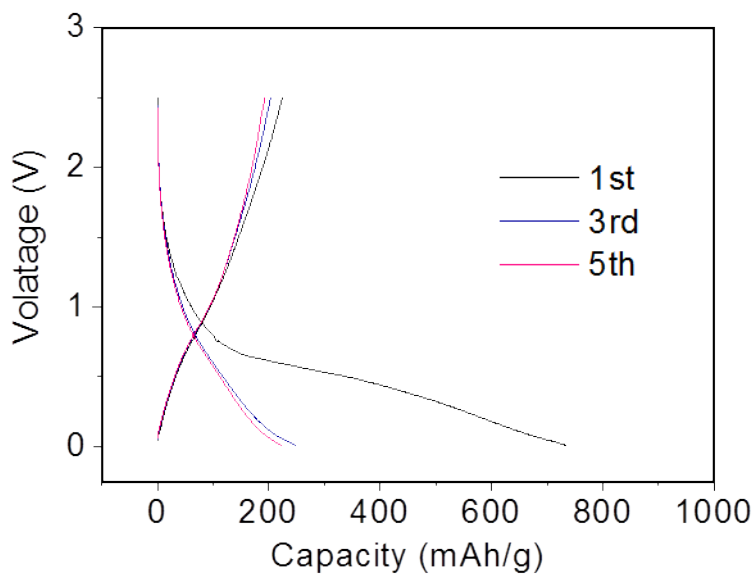


Fig. S10 shows the cycle performance of graphene (G) and NCG samples. The results show that the NCG has more stable cycle performance than the graphene at a current density of 25 mA g⁻¹. The pores serve as open channels for movement of Na ions and nitrogen-doping gives better conductivity than that of the graphene.

Fig. S11 Charge-discharge profile of TNCG samples between 0.01 and 2.5V.



The electrode shows the charge and discharge profiles of the TNCG at a current density of 50 mA g⁻¹ between 0.01 and 2.5V. The specific charge capacity of the first cycle is 224mAh g⁻¹, which is higher than the other reported values for Na-ion batteries based on an intercalation reaction such as amorphous TiO₂ (150 mAh g⁻¹ at a current density of 50 mA g⁻¹)⁴, Na₂Ti₃O₇ (177 mAh g⁻¹ at a current density of 35.6 mA g⁻¹)⁵, and Li₄Ti₅O₁₂ (125 mAh g⁻¹ at a 0.2 C rate)⁶.

References

1. W. S. Hummers Jr and R. E. Offeman, *J Am Chem Soc*, 1958, **80**, 1339-1339.
2. Z Fan, Q Zhao, T Li, J Yan, Y Ren, J Feng, T Wei, *Carbon*, 2012, **50**, 1699–1703.
3. M.-S. Song, A. Benayad, Y.-M. Choi and K.-S. Park, *Chem. Commun.*, 2011, **48**, 516-518.
4. H. Xiong, M. D. Slater, M. Balasubramanian, C. S. Johnson and T. Rajh, *J Phys Chem Lett*, 2011, **2**, 2560-2565.
5. A. Rudola, K. Saravanan, C. W. Mason and P. Balaya, *J Mater Chem A*, 2013, **1**, 2653-2662.
6. Y. Sun, L. Zhao, H. Pan, X. Lu, L. Gu, Y.-S. Hu, H. Li, M. Armand, Y. Ikuhara and L. Chen, *Nature communications*, 2013, **4**, 1870.